ARTICLE

Robust and Durable Triboelectric Nanogenerators Enabled by Mechanically Strong and Mildly Healable Polymer

Received 00th January 20xx,
Accepted 00th January 20xx

DOI: 10.1039/x0xx00000x

Wei Xu [a,b,d], Hongzhen Liu [b], Man-Chung Wong [c], Huimin He [b], Jianhua Hao [c], Lizhi Xu* [a,b]

Capabilities in healing structural damages are highly desired for triboelectric nanogenerators (TENGs), which are subject to repeated mechanical loadings. However, it remains difficult to balance the intrinsic mechanical strength and healing capability of the materials used in TENGs. Herein, we exploit a mechanically strong and mildly healable polymer (THP) as the key material of TENGs. The THP is based on polyurethane–urea containing coordinate bonds, and its healing can be triggered by simply wetting the breakage area with water or alcoholic drinks. The healing ratio and the tensile strength of the THP can reach ~90 % and ~11.6 MPa, respectively. Correspondingly, the prepared THP-based TENGs (THP-TENGs) exhibit high robustness to withstand mechanical loadings as well as excellent healability for recovering device functionalities after mechanical damage. In addition, disused devices can be recycled to produce new ones based on the solution processibility of THP. The fabricated THP-TENG could serve as mechanical energy harvester as well as the self-powered sensors for detecting tactile and electrophysiological signals, suggesting utilities in advanced wearable systems.

Introduction

The rapid development of wearable electronics and internet of thing imposes high requirements on power sources and sensors.[1-3] Triboelectric nanogenerator (TENG), a device based on triboelectric effect and electrostatic induction, possesses excellent ability to convert ambient mechanical energy into electrical output in a miniaturized configuration. This device shows great potential as distributed power source for emerging electronics or acting as self-powered sensors for detecting mechanical motions.[3-7] Compared to other miniaturized energy devices, TENG possesses various advantages, including simple structure, low cost, high output voltage, and high efficiency in energy conversion for low-frequency mechanical inputs.[8-12]

During the process of energy harvesting, TENGs are subject to frequent mechanical forces for generating electrical output. This process could cause mechanical damage to the device structures, leading to reduced durability and lifespan of the system.[13, 14] A promising method to solve this problem is to construct healable TENGs based on appropriate reconfigurable polymer materials.[14-16] However, there is a tradeoff between mechanical strength and healability for most healable polymers, which create challenges for their utilization in TENGs.[17-23] For instance, autonomous-healable polymers with high molecular chain mobility can heal without external trigger. But they usually present relatively low mechanical strength, which cannot withstand the high mechanical loadings applied on TENGs.[24-29] On the other hand, devices based on non-autonomous-healable polymers, as exemplified by polymers containing Diels–Alder bonds etc., could easily exhibit considerable mechanical strength at the level of above 10 MPa. But their healing may require sophisticated conditions, such as high temperature, infrared radiation, or other stimuli that are not compatible with the device system.[15, 19, 30, 31] In this regard, simplicity of the healing process aligned with the normal operating condition of TENGs becomes essential. Despite extensive efforts, technological approaches that can achieve these attributes remain limited.

In this study, we exploit a mechanically strong and mildly healable polymer (THP) as the base material for the construction of TENGs. The THP is constructed from polyurethane–urea and involves coordination interactions. The tensile strength of the THP (11.6 MPa) outperforms most of healable polymers used in TENGs, which confers excellent robustness on the devices. The healing of THP can be conducted in the presence of water or alcoholic drinks which are ubiquitous and common in daily life. After healing of mechanically damaged devices, the electrical output of the THP-based TENG (THP-TENG) can recover to the initial state and remain stable for 8000 operation cycles. Furthermore, based on the solvent processability of THP, disused THP-TENGs can be recycled for the production of new devices. The fabricated THP-TENG can serve as the mechanical energy harvester and the self-powered sensors for detecting tactile and electrophysiology signals simultaneously, suggesting opportunities for applications in wearable electronic systems.

Experimental Section

[a] Advanced Biomedical Instrument Centre Limited, Hong Kong, China.
[b] Department of Mechanical Engineering, The University of Hong Kong, Hong Kong, China
[c] Department of Applied Physics, The Hong Kong Polytechnic University, Hong Kong, China.
[d] Research Centre for Humanoid Sensing, Zhejiang Lab, Hangzhou, China.
Electronic Supplementary Information (ESI) available: [details of any supplementary information available should be included here].

Reagents and Materials:

Polytetrahydrofuran (PTMEG, Mn = 850), Isophorone diisocyanate (IPDI), dibutyltin dilaurate (DBTDL), triethylamine (TEA), Dopamine hydrochloride (DA-HCl), dimethylformamide (DMF), and calcium chloride ($CaCl_2$) were purchased from Aladdin-reagent (China). All the chemicals were used as received.

Preparation of the mechanically tough and mildly healable polymer (THP):

30 g PTMEG was heated in oil bath of about 115 °C under vacuum and magnetic stirring for 2 hr for water removal. After cooling the system to 70 °C, 16.3 g IPDI and 2 drops of DBTDL were added under mechanical stirring for sealed reaction. The temperature of the oil bath was successively raised to 105 °C for 3 h and 115 °C for 1 hr to form the isocyanate terminated prepolymer (NCO-prepolymer) for further experiment. 5 g NCO-prepolymer disslolved in 5ml DMF and 1.05 g DA-HCl dissolved in 4 ml DMF were mixed. Then 0.6 g TEA was added in two batches in 2 hr followed by reaction for 24 hr to get the catechol containing prepolymer (DA-NCO-prepolymer). Then, the catechol terminated prepolymer (DA-prepolymer) was obtained after the separation and precipitation in water for several times during 1-2 hr. The DA-prepolymer was dissolved into DMF (20 ml) by means of the stirring under 90 °C. Then 0.126 g $CaCl_2$ dissolved in 5 mL DMF by sonicator was added for mixing for 30 min. The mixture solution was transferred to a Teflon dish for the chain extension and evaporation of the solvent at 65 °C for 2 days. The resultant THP film was obtained for the fabrication of TENGs.

Preparation of the THP-TENG:

THP based TENG (THP-TENG) was fabricated by encapsulating electrodes between two THP layers. Specifically, the electrode pattern was prepared by coating Ag paste on a Teflon film through a stencil mask followed by heating and removing the solvent. Then the surface of a THP film was wetted by the ethanol, and the resultant sticky THP surface can transfer electrode pattern from Teflon surface to THP surface. A Ni fabric tape was used to connect the electrode with external circuit for measurement. The THP-TENG was achieved after encapsulating the electrode with another THP layer. For detecting the electromyography signals, another electrode pattern was fabricated and transferred to the bottom surface of the THP-TENG in a similar way.

Measurement of the device:

The output voltage and current were characterized by LeCroy WaveRunner Oscilloscope (probe resistance value of 50 MΩ) and low noise current amplifier (Stanford Research Systems, SR570), respectively. The tensile property of the prepared polymer was measured by a universal testing machine at room temperature of about 24-27 °C and humidity of ~50 %. The healing ratio was measured by tensile curves. During the healing process, the cutting width and depth are around 0.7 cm and 0.4 mm, respectively. The added amount of water is about 100 μL. The water was added in twice. The voltage-current (*I-V*) curves were measured by electrochemical workstation. The electromyogram (EMG) signals was measured by data acquisition hardware device (PowerLab26T).

Results and discussion

To achieve the expected TENG devices, the mechanically strong and mildly healable polymer (THP) was firstly prepared as the base materials of the device. As illustrated in Figure 1, the synthesis process of THP mainly includes four steps: (1) Synthesis of the isocyanate terminated prepolymer (NCO-prepolymer) by the reaction of polytetrahydrofuran (PTMEG) and isophorone diisocyanate (IPDI). (2) Synthesis of the catechol containing prepolymer (DA-NCO-prepolymer) by the reaction between NCO-prepolymer and the dopamine (molar ratio of isocyanate to catechol ends is about 1 to 0.7, and TEA was excessive). (3) Chain extension of DA-NCO-prepolymer by the reaction between water and -NCO to form the catechol terminated prepolymer (DA-prepolymer). The structure of product was confirmed by the 1H NMR (Figure S1) and the UV-VIS absorption spectroscopy (Figure S2). (4) Chain extension of DA-prepolymer by the coordination interaction between catechol ends and Ca^{2+}. The coordination was proved by isothermal titration calorimetry (Figure S3). The final THP film was formed after removing the solvent. The existence of both isocyanate and catechol ends in DA-NCO-prepolymer enables the two-step chain-extension reaction to reach the excellent comprehensive performance. The first chain extension using water generates urea groups for the improvement of mechanical strength. The second chain extension using Ca^{2+} introduces dynamic coordination bonds for further enhancing the strength of THP and endowing the healability.

As the constituent material of TENGs, the mechanical property of THP strongly affects the robustness of devices. Figure 2a shows the tensile stress-strain curves of THP samples with different amount of added $CaCl_2$ ($C_{Ca,}$ which is defined as the mole percentage ratio of catechol coordinated with Ca^{2+} to the total catechol). It was found that the tensile strength of THP improves with the increment of C_{Ca}. For the sample without added $CaCl_2$, the tensile strength was about 4.8 MPa. After adding 14 % $CaCl_2$ into the system, the resultant THP sample exhibits an increased tensile strength of 6.3 MPa. When the C_{Ca} enhances to 28 % and 42 %, the tensile strength of THP can arrive at 11.6 MPa and 19.7 MPa, respectively, which are higher than that of most healable polymers used in TENGs. As aforementioned, by means of the chain extension of DA-NCO-prepolymer using water, the tensile strength of the prepared DA-prepolymer can arrive at 4.8 MPa already. The introduction of $CaCl_2$ contributes to the further chain extension of DA-prepolymer, thereby leading to the declined molecular mobility and the improved strength of THP.[32, 33]

The mechanical property of THP was further evaluated by cyclic tensile tests as shown in Figure 2b and Figure S4. After a strain of 50 % was applied, relatively large stress–strain loops are observed. Specifically, when the strain arrives at about 10 %, the yield point appears accompanying with the rupture of some intermolecular bonds and hard-segment phase. During the unloading process, the large residual strain is observed, which can be attributed to the chain entanglement and the reconfiguration of some hydrogen bonds and coordinate bonds etc.. After annealing the cyclically tested sample without

mechanical loading for 1 hr, followed by cyclic testing, the sample exhibit loops (cycle 5 and after in Figure 2b) similar to the previous cycles, indicating the partly recovery of molecular structure driven by entropic elasticity. From the perspective of devices, it is necessary to further develop THP with low hysteresis. Some strategies, such as the optimization of the soft and hard segments, and the construction of dynamic crosslinked structure etc., have been reported and deserve attempts.[34-36] In addition, the mechanical property was also characterized by Dynamic Mechanical Analysis (DMA) as shown in Figure S5, where multiple transition temperatures are observed.

The as-prepared THP shows healing ability in the presence of water, and the healing process is illustrated in Figure 2c. Specifically, the THP sample (C_{Ca}=28 %) was firstly cut using a razor blade (i-ii). After re-contacting the cut ends carefully and adding a small amount of water on the breakage area, a piece of scotch tape was applied on the breakage area for retaining the wetting of this area for 1 day (iii). Then the scotch tape was removed, and the healed THP sample without a scar was achieved after the evaporation of water (iv). Optical microscope images of the breakage area show that the breakage mark (v) almost disappeared after the water-assisted healing treatment (vi), confirming the healing ability of the prepared THP.

The healability of THP can be quantitatively measured by comparing the tensile stress-strain curves of samples at the initial and the healed state, and the healing ratio is defined as the proportion of the failure strain of healed sample relative to that of initial one. As shown in Figure 2d, the failure strain of the initial THP (C_{Ca}=28 %) and the healed THP (water treatment for 1 day) are 317 % and 297 %, respectively. Correspondingly, the healing ratio of THP was calculated as above 90 %. In contrast, the healing ratio of THP healed without application of water was only 6.6 %, implying the importance of water in the healing process. The introduction of water not only enables the coordination between Ca^{2+} and catechol to become dynamic, but also plasticizes the polymer system.[37-39] Both factors lead to the increased molecular mobility of THP, promoting the diffusion of molecular chains and the structure re-establishment around breakage area for final healing.

Figure 2e demonstrates the healing ratio of prepared THP samples with different C_{Ca} (water treatment for 1 day). The results show that the healing ratio decreases with the increase of the C_{Ca}. When the C_{Ca} increases from 14 % to 42 %, the healing ratio of samples changes from 94 % to 52 %. As aforementioned, the introduction of $CaCl_2$ mainly contributes to the chain extension of DA-prepolymer. This means that the THP samples with higher C_{Ca} possesses the larger length of molecular chains and therefore lower molecular mobility, leading to the decrease in healability. Besides water, the healing of THP can also be triggered by some alcohol drinks, such as whisky. It was found that the sample healed by whisky shows better healing ratio than the sample healed by water when healing time is short (1.5 hr), which may be attributed to the better compatibility of alcohol with THP.

From the perspective of practical operation, healable TENG is expected to possess not only the healability for fracture recovery, but also excellent strength to resist mechanical failure. Figure 2f and Figure S6 summarizes the mechanical strength and the healing ratio of a series of healable polymers used in TENGs.[15, 19, 27-29, 31, 40-49] It was found that our THP shows an obviously higher strength than numerous autonomous-healable polymers used in TENGs. The strength of THP is comparable to that of non-autonomous-healable polymers. However, the healing of regular non-autonomous-healable materials usually requires stimuli that are not compatible with operation environment of TENGs, such as heat or infrared radiation etc. These processes are inconvenient when the devices are used in an outdoor or wearable configuration. In contrast, the prepared THP can conduct the healing easily with the assistance of water or alcoholic drinks which are ubiquitous, mild, and safe. This highlights the advantage of THP as the base material of TENGs, which balances the healing and mechanical properties. Besides, this strategy could be compatible to other polymer systems to achieve various mechanically strong and mildly healable polymers serving for the development of advanced healable TENGs.

Based on the THP, we prepared a single-electrode-mode TENG (THP-TENG) which consists of external THP layers and an internal electrode as shown in Figure 3a. The THP-TENG can convert mechanical energy into electricity based on the triboelectric effects, and the working principle can be illustrated in Figure 3a (iii-vi). Specifically, the contact between the paired material and the THP-TENG causes electron transfer and re-distribution at the contact interface because of their difference in electron affinity (iii). When the paired material departs from the device, two oppositely charged surfaces are generated. Among them, the charged THP surface will induce a transient electron flow between the internal electrode and the ground by electrostatic effects (iv) until the electrical equilibrium is achieved (v). When the charged paired material approaches to the device again, the opposite electric potential and electron flow are induced (vi). By repeating this procedure driven by mechanical force, the ambient mechanical energy is successfully converted.

The paired contact material in Figure 3a could be any material that possesses different electron affinity with the THP. Herein, we take PDMS film as an example of the paired material to evaluate the electrical output performance of the THP-TENG. As shown in Figure 3b and c, when the THP-TENG (2.5 cm × 4 cm) is driven by a linear motor with the frequency of 4 Hz, the peak output voltage and short-circuit current (I_{sc}) of device are about 28 V and 2.86 μA, respectively. The output voltage and current change under different load resistance is shown in Figure 3d. The peak electrical power density is calculated as about 2.9 mW/m^2 at a load resistance of 100 MΩ (Figure 3e). Both the type of paired materials and the contact frequency will affect the electrical output of device. As shown in Figure 3f, the PDMS as the paired material could achieve a relatively high output voltage, which is ascribed to its high electron affinity compared with other materials. Meanwhile, it was found that output voltage increases with the enhancement of contact frequency from 1 Hz to 8 Hz (Figure 3g), which is in accordance with the previous report.[50-53]Additionally, after introducing an inverter

into the circuit, the AC signals can be transferred into DC electrical output for charging capacitors. The voltage of the capacitor (18 μF) arrived at about 1.87 V after being charged by a THP-TENG for 10 min as shown in Figure 3h.

The prepared device can also serve as self-powered sensors for detecting external stimuli. As shown in Figure 4a (i), we fabricated a THP-TENG with an array of square-shaped electrodes as a self-powered tactile sensor. It was found that when a finger slides on the surface of the device (e.g. the area in the red box in Figure 4b), only those electrodes under the contact area (electrodes 1-3, Figure 4b) generate significant electric signals as shown in Figure 4c. This is because that the triboelectric charges created from finger touching are localized and create maximum electrical output through the nearest electrode based on the electrostatic effect. Correspondingly, the THP-TENG can distinguish the location of external mechanical stimuli by measuring the electrical output signals of different electrodes. Furthermore, adding an additional pair of electrodes (Figure 4a (ii)) at the bottom surface of the THP-TENG (Figure 4a (i)) creates independent channels (Figure 4a (iii)) for the measurement of electrophysiological signal.[54] To demonstrate the functionality, we attached these devices on the medial and lateral forearm of a health volunteer, respectively (Figure S7), for collecting electromyography (EMG) signals. When three distinct gestures are made, distinguishable filtered EMG patterns are obtained from the bottom electrode pair of the devices (Figure 4d). Correspondingly, the THP-TENG shows the potential for gestures recognition. To our knowledge, few attempts have been made in constructing healable devices with both mentioned functions.

As shown in Figure 5a, the healing of THP-TENG can be conducted by simply covering a piece of scotch tape on the wetted breakage area, which is very convenient and safe to operate in daily application. In addition to the healing of device structures, the recovery of conductivity of the electrode was observed. As shown in Figure 5b (iii), the electrode was in a high-resistance state when it was cut apart, where the voltage across the electrode approximates to the open-circuit voltage (V_{oc}). Its conductivity restored to the original value by healing of the THP layer. Correspondingly, the extinct LED light (Figure 5b (i)) connected in series with the electrode is lit up again (Figure 5b (ii)). Attributed to the recovery of electrodes' conductivity, restoration of the electrical output of THP-TENG is realized, and the output voltage of the healed device can restore to the initial value of about 28 V as shown in Figure 5c. It was also found that the healed device can stand a long-term and continuous operation for 8000 cycles without performance degradation as shown in Figure 5d. The THP-TENG also shows recyclability due to the solution processability of THP. As shown in Figure 5e, the discarded device (i) can be broken into small pieces (ii) and then dissolved into DMF (iii). After centrifuging, the Ag electrode portion is separated from the system (iv), and the THP film can be formed again after evaporating the solvent of the supernatant (v). This recyclability endows the device with the economic and environmental friendliness for further application.

Conclusion

In this study, we developed a mechanically strong and mildly healable polymer, namely THP, as the base material of TENGs. The tensile strength of THP (C_{Ca}=28%) can reach 11.6 MPa, and the healing of THP can be easily conducted with the assistance of water or alcohol drinks with the healing ratio of about 90 %. TENGs based on THP are mechanically robust and also healable in a mild condition that is convenient in daily operation. After healing structural damages, the output voltage of the device can recover to the initial state, and the healed device shows stable performance during continuous operation for 8000 cycles without performance decay. In addition, the THP-TENG also possesses solution processability for devices recycling. The prepared THP-TENG shows potential as the mechanical energy harvester and the self-powered sensors for detecting tactile and electromyographic signals, indicating possibilities for the development of advanced soft electronics with improved mechanical resilience.

Conflicts of interest

There are no conflicts to declare.

Acknowledgements

The study is supported by Research Grants Council (RGC), University Grants Committee (UGC) (Project 17200722 and 17200320 to L.X).

Notes and references

1. J. Li, C. Wu, I. Dharmasena, X. Ni, Z. Wang, H. Shen, S. L. Huang and W. Ding, *Intell. Converged Networks*, 2020, **1**, 115-141.
2. Z. L. Wang, *Adv. Energy Mater.*, 2020, **10**, 2000137.
3. W. Liu, Z. Wang and C. Hu, *Mater. Today*, 2021, **45**, 93-119.
4. Y. Zhou, M. Shen, X. Cui, Y. Shao, L. Li and Y. Zhang, *Nano Energy*, 2021, **84**, 105887.
5. J. Luo and Z. L. Wang, *EcoMat*, 2020, **2**, e12059.
6. Z. L. Wang, J. Chen and L. Lin, *Energy Environ. Sci.*, 2015, **8**, 2250-2282.
7. J.-H. Zhang, Z. Li, J. Xu, J. Li, K. Yan, W. Cheng, M. Xin, T. Zhu, J. Du, S. Chen, X. An, Z. Zhou, L. Cheng, S. Ying, J. Zhang, X. Gao, Q. Zhang, X. Jia, Y. Shi and L. Pan, *Nat. Commun.*, 2022, **13**, 5839.
8. L. Zhou, D. Liu, J. Wang and Z. L. Wang, *Friction*, 2020, **8**, 481-506.
9. Z. L. Wang, T. Jiang and L. Xu, *Nano Energy*, 2017, **39**, 9-23.
10. C. Wu, A. C. Wang, W. Ding, H. Guo and Z. L. Wang, *Adv. Energy Mater.*, 2019, **9**, 1802906.
11. W. Xu, L.-B. Huang, M.-C. Wong, L. Chen, G. Bai and J. Hao, *Adv. Energy Mater.*, 2017, **7**, 1601529.
12. J.-H. Zhang, Y. Li, J. Du, X. Hao and H. Huang, *J. Mater. Chem. A*, 2019, **7**, 11724-11733.
13. W. Xu, M.-C. Wong and J. Hao, *Nano Energy*, 2019, **55**, 203-215.
14. W. Xu, L.-B. Huang and J. Hao, *Nano Energy*, 2017, **40**, 399-407.

15. W. Xu, M.-C. Wong, Q. Guo, T. Jia and J. Hao, *J. Mater. Chem. A*, 2019, **7**, 16267-16276.
16. J. Jiang, Q. Guan, Y. Liu, X. Sun and Z. Wen, *Adv. Funct. Mater.*, 2021, **31**, 2105380.
17. S. Nevejans, N. Ballard, M. Fernández, B. Reck, S. J. García and J. M. Asua, *Polymer*, 2019, **179**, 121670.
18. C. Kim and N. Yoshie, *Polym. J.*, 2018, **50**, 919-929.
19. B.-X. Cheng, C.-C. Lu, Q. Li, S.-Q. Zhao, C.-S. Bi, W. Wu, C.-X. Huang and H. Zhao, *J. Polym. Environ.*, 2022, DOI: 10.1007/s10924-022-02586-z.
20. Y. Yang and M. W. Urban, *Chem. Soc. Rev.*, 2013, **42**, 7446-7467.
21. K. Parida, J. Xiong, X. Zhou and P. S. Lee, *Nano Energy*, 2019, **59**, 237-257.
22. N. Mohd Kanafi, A. Abdul Ghani, N. Abdul Rahman, A. Abd Aziz and S. M. Sapuan, *J. Mater. Sci.*, 2023, **58**, 608-635.
23. Y. Li, Y. Jin, W. Zeng, R. Zhou, X. Shang, L. Shi, L. Bai and C. Lai, *Prog. Org. Coat.*, 2023, **174**, 107256.
24. U. Gulyuz and O. Okay, *Macromolecules*, 2014, **47**, 6889-6899.
25. S. Terryn, J. Langenbach, E. Roels, J. Brancart, C. Bakkali-Hassani, Q.-A. Poutrel, A. Georgopoulou, T. George Thuruthel, A. Safaei, P. Ferrentino, T. Sebastian, S. Norvez, F. Iida, A. W. Bosman, F. Tournilhac, F. Clemens, G. Van Assche and B. Vanderborght, *Mater. Today*, 2021, **47**, 187-205.
26. B. Willocq, J. Odent, P. Dubois and J.-M. Raquez, *RSC Adv.*, 2020, **10**, 13766-13782.
27. Y.-C. Lai, H.-M. Wu, H.-C. Lin, C.-L. Chang, H.-H. Chou, Y.-C. Hsiao and Y.-C. Wu, *Adv. Funct. Mater.*, 2019, **29**, 1904626.
28. Y. Du, X. Wang, X. Dai, W. Lu, Y. Tang and J. Kong, *Journal of Materials Science & Technology*, 2022, **100**, 1-11.
29. X. Dai, L.-B. Huang, Z. Sun, Y. Du, B. Xue, M.-C. Wong, J. Han, Q. Liang, Y. Wu, B. Dong, J. Kong and J. Hao, *Mater. Horiz.*, 2022, **9**, 2603-2612.
30. N. Yoshie, S. Yoshida and K. Matsuoka, *Polym. Degrad. Stab.*, 2019, **161**, 13-18.
31. Q. Guan, Y. Dai, Y. Yang, X. Bi, Z. Wen and Y. Pan, *Nano Energy*, 2018, **51**, 333-339.
32. D. G. Barrett, D. E. Fullenkamp, L. He, N. Holten-Andersen, K. Y. C. Lee and P. B. Messersmith, *Adv. Funct. Mater.*, 2013, **23**, 1111-1119.
33. W. L. Peng, Z. P. Zhang, M. Z. Rong and M. Q. Zhang, *ACS Appl. Mater. Interfaces*, 2020, **12**, 27614-27624.
34. Y. Wang, X. Yu, H. Zhang, X. Fan, Y. Zhang, Z. Li, Y.-E. Miao, X. Zhang and T. Liu, *Macromolecules*, 2022, **55**, 7845-7855.
35. D. Fu, W. Pu, Z. Wang, X. Lu, S. Sun, C. Yu and H. Xia, *J. Mater. Chem. A*, 2018, **6**, 18154-18164.
36. W. Kong, Y. Yang, Y. Wang, H. Cheng, P. Yan, L. Huang, J. Ning, F. Zeng, X. Cai and M. Wang, *J. Mater. Chem. A*, 2022, **10**, 2012-2020.
37. J. Li, H. Ejima and N. Yoshie, *ACS Appl. Mater. Interfaces*, 2016, **8**, 19047-19053.
38. S. Xu, D. Sheng, X. Liu, F. Ji, Y. Zhou, L. Dong, H. Wu and Y. Yang, *Polym. Int.*, 2019, **68**, 1084-1090.
39. N. N. Xia, X. M. Xiong, J. Wang, M. Z. Rong and M. Q. Zhang, *Chem. Sci.*, 2016, **7**, 2736-2742.
40. P. Liu, N. Sun, Y. Mi, X. Luo, X. Dong, J. Cai, X. Jia, M. A. Ramos, T. S. Hu and Q. Xu, *Compos. Sci. Technol.*, 2021, **208**, 108733.
41. H. Chen, J. J. Koh, M. Liu, P. Li, X. Fan, S. Liu, J. C. C. Yeo, Y. Tan, B. C. K. Tee and C. He, *ACS Appl. Mater. Interfaces*, 2020, **12**, 31975-31983.
42. T. Patel, M. P. Kim, J. Park, T. H. Lee, P. Nellepalli, S. M. Noh, H. W. Jung, H. Ko and J. K. Oh, *ACS Nano*, 2020, **14**, 11442-11451.
43. R. Liu, Y. Lai, S. Li, F. Wu, J. Shao, D. Liu, X. Dong, J. Wang and Z. L. Wang, *Nano Energy*, 2022, **95**, 107056.
44. X. Dai, L.-B. Huang, Y. Du, J. Han, Q. Zheng, J. Kong and J. Hao, *Adv. Funct. Mater.*, 2020, **30**, 1910723.
45. H. Li, F. Xu, T. Guan, Y. Li and J. Sun, *Nano Energy*, 2021, **90**, 106645.
46. Z. Wu, J. Chen, D. W. Boukhvalov, Z. Luo, L. Zhu and Y. Shi, *Nano Energy*, 2021, **85**, 105990.
47. C. Li, P. Wang and D. Zhang, *Nano Energy*, 2023, **109**, 108285.
48. M. Burnworth, L. Tang, J. R. Kumpfer, A. J. Duncan, F. L. Beyer, G. L. Fiore, S. J. Rowan and C. Weder, *Nature*, 2011, **472**, 334-337.
49. Y. Jia, L. Zhang, M. Qin, Y. Li, S. Gu, Q. Guan and Z. You, *Chem. Eng. J.*, 2022, **430**, 133081.
50. L. B. Huang, G. X. Bai, M. C. Wong, Z. B. Yang, W. Xu and J. H. Hao, *Adv. Mater.*, 2016, **28**, 2744-2751.
51. L.-b. Huang, W. Xu, G. Bai, M.-C. Wong, Z. Yang and J. Hao, *Nano Energy*, 2016, **30**, 36-42.
52. J. Luo, Y. Su, C. Zhang, Y. Gu, A. Liu, Z. Li, W. Feng and K. Zhao, *Nano Energy*, 2022, **103**, 107859.
53. Y. Pang, X. Xu, S. Chen, Y. Fang, X. Shi, Y. Deng, Z.-L. Wang and C. Cao, *Nano Energy*, 2022, **96**, 107137.
54. K. Zhu, W. Guo, G. Yang, Z. Li and H. Wu, *ACS Appl. Electron. Mater.*, 2021, **3**, 1350-1358.

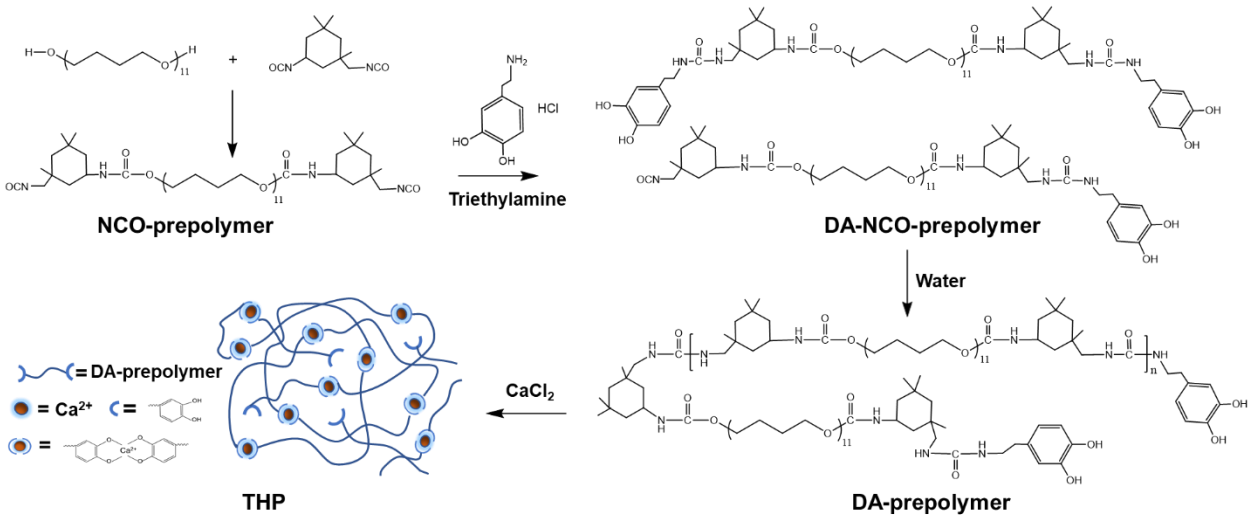

Figure 1. The preparation process of THP.

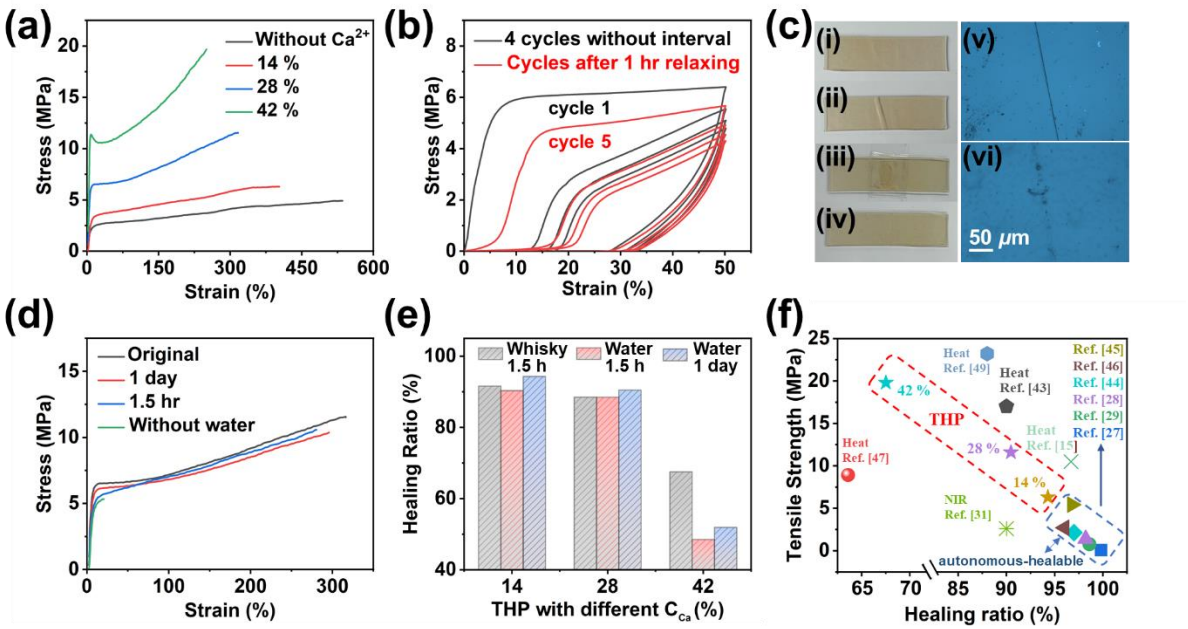

Figure 2. The mechanical and healable properties of THP. (a) Tensile stress-strain curves of THP samples with different C_{Ca}. (b) Cyclic tensile tests of THP with C_{Ca} of 28 %. (c) Photographs (i-iv) and microscope images (v-vi) illustrating the water-assisted healing process of THP. (d) The tensile stress-strain curves of THP at the original and the healed state. (e) The healing ratio of THP (C_{Ca}=14 %, 28% and 42 %) under different healing treatment. (f) Comparison in healing ratio and tensile strength of representative healable polymers employed in TENGs. Among them, the data in blue circle come from some previously reported autonomous-healable TENGs, and the data in red circle come from our THP with C_{Ca} of 14 %, 28 % and 42 %. The others come from some previously reported non-autonomous-healable TENGs.

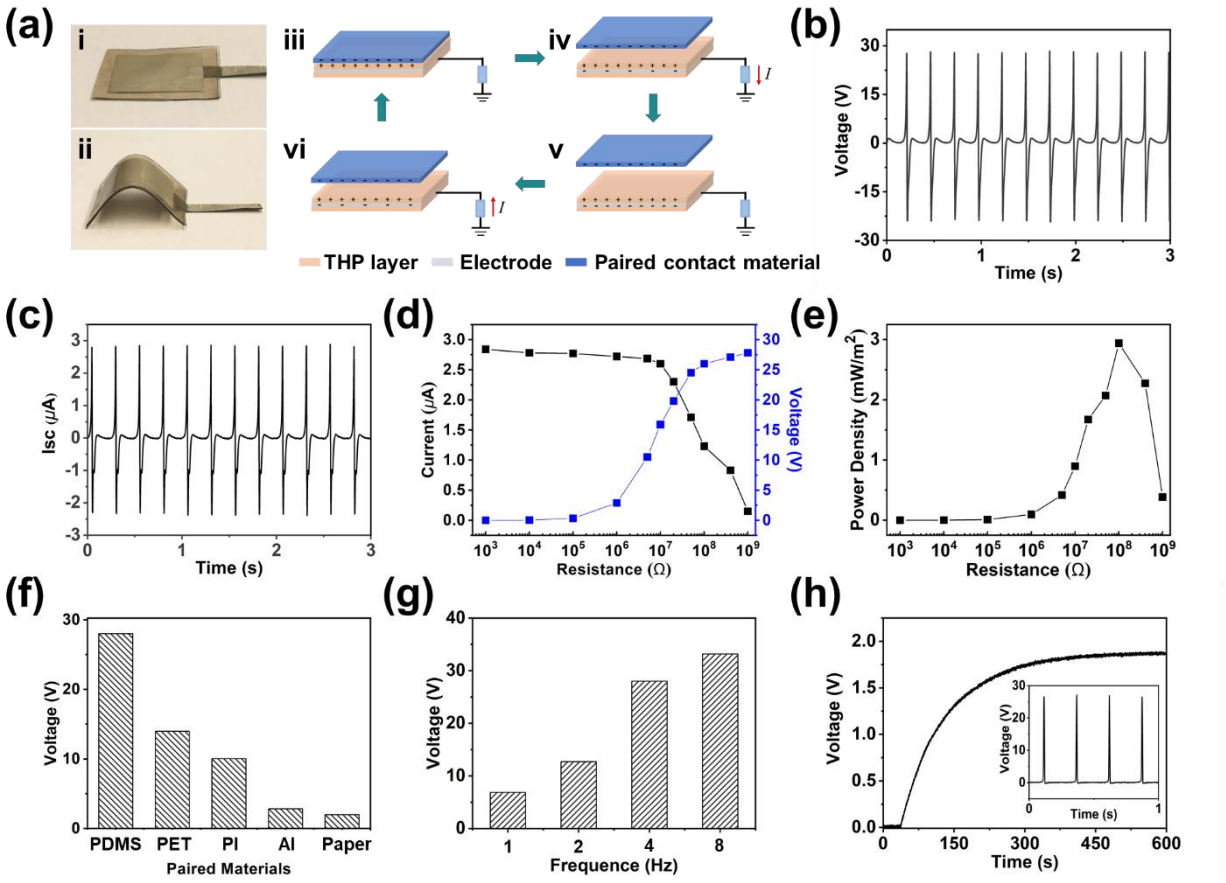

Figure 3. The electrical performance of THP-TENG. (a) Photographs (i-ii) and the working principle (iii-vi) of THP-TENG. (b-c) Open-circuit voltage (b) and short-circuit current (c) of THP-TENG driven by a linear motor. (d) Output voltage and current with various resistance. (e) Output power density with various resistance. (f-g) Open-circuit voltage of the device under different paired contact materials (f) and contact frequencies (g). (h) The change in voltage of an 18-μF capacitor when charged by a THP-TENG, with the inset showing the DC electrical output of the THP-TENG combined with an inverter into the circuit.

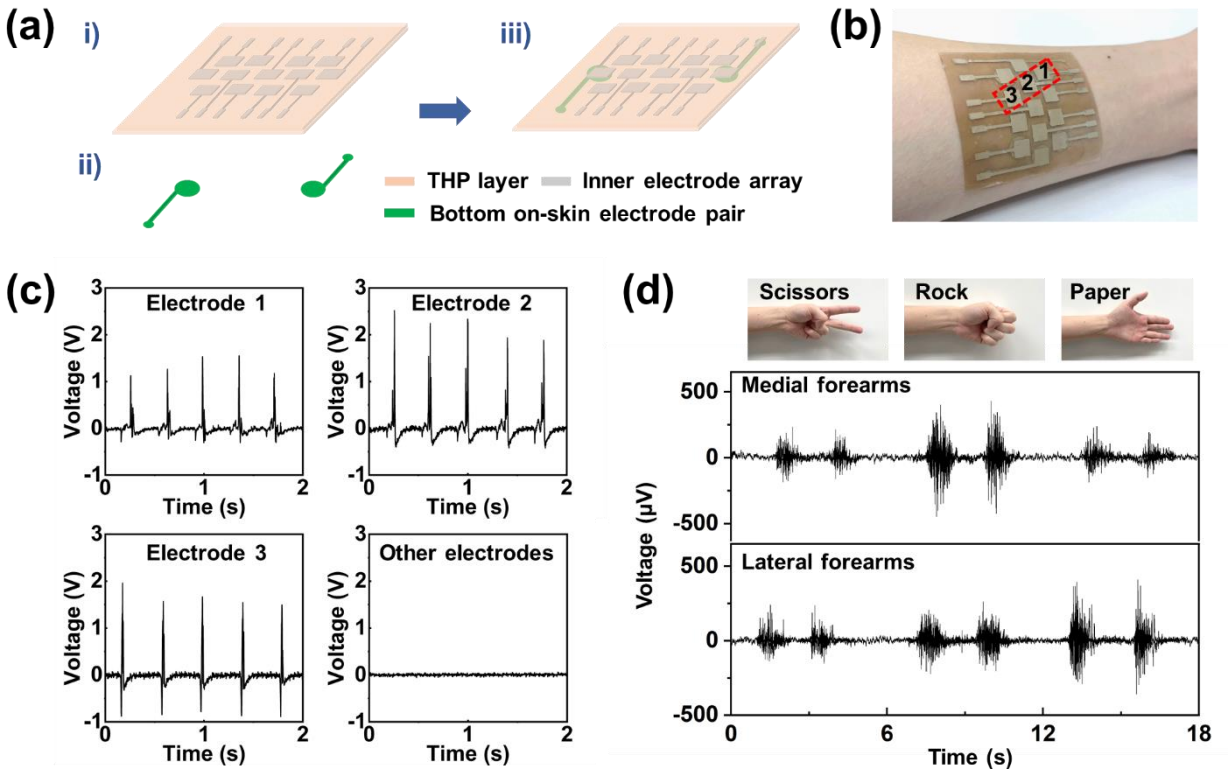

Figure 4. The sensing performance of THP-TENG in detecting tactile and electrophysiological signal. (a) Schematics of a THP-TENG including square-shaped inner electrodes array and circle-shaped on-skin electrode pair on the bottom surface. (b) A photograph of the THP-TENG attached on the medial forearm. (c) Electrical signals generated from different square-shaped inner electrodes when a finger slides on the surface of the device. (d) Three distinct gestures and the corresponding filtered EMG signals collected from the bottom electrode pair of two devices attached on the medial and the lateral forearm, respectively.

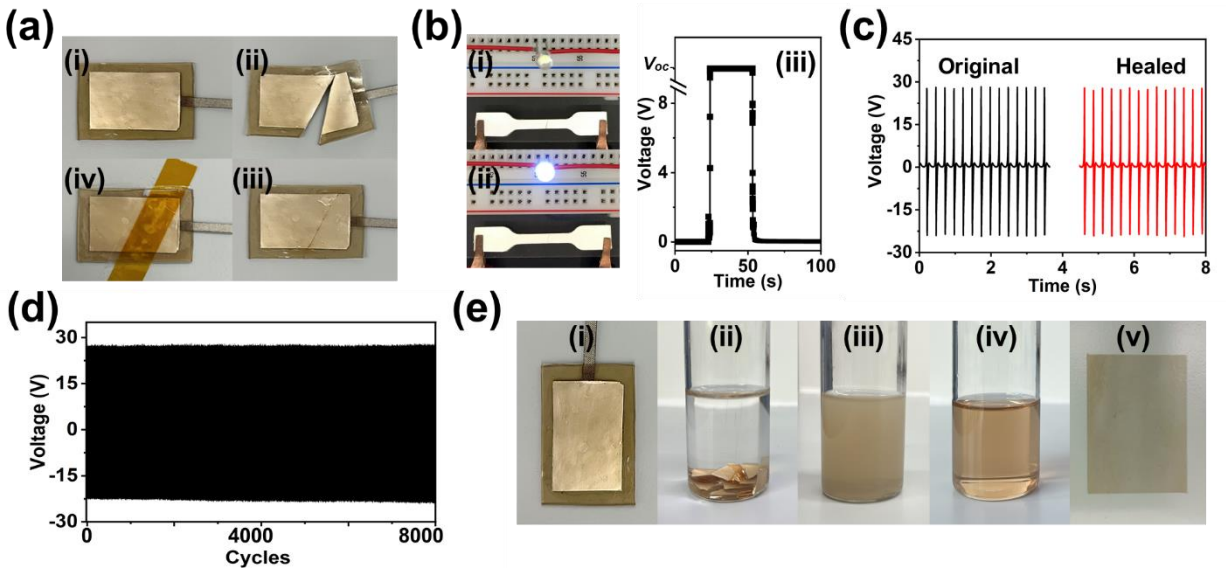

Figure 5. The healing and recycling performance of the device. (a-c) Healing of the device integrity (a), electrical conductivity of the electrode (b), and the output voltage of the device (c). (d) The open-circuit voltage output of the healed THP-TENG during the continuous operation for 8000 cycles. (e) The recycling process of THP-TENG using DMF solvent.